5-2003

A Simulation Model for the Four-Phase Switched-Reluctance Motor

James T. Cox
University of Tennessee - Knoxville

To the Graduate Council:

I am submitting herewith a thesis written by James T. Cox entitled "A Simulation Model for the Four-Phase Switched-Reluctance Motor." I have examined the final electronic copy of this thesis for form and content and recommend that it be accepted in partial fulfillment of the requirements for the degree of Master of Science, with a major in Electrical Engineering.

Jack Lawler, Major Professor

We have read this thesis and recommend its acceptance:

Paul B. Crilly, Syed Islam

Accepted for the Council:
Carolyn R. Hodges

Vice Provost and Dean of the Graduate School

(Original signatures are on file with official student records.)

To the Graduate Council:

I am submitting herewith a thesis written by James T. Cox entitled “A Simulation Model for the Four-Phase Switched-Reluctance Motor.” I have examined the final electronic copy of this thesis for form and content and recommend that it be accepted in partial fulfillment of the requirements for the degree of Master of Science, with a major in Electrical Engineering.

Jack Lawler
Major Professor

We have read this thesis and
recommend its acceptance:

Paul B. Crilly

Syed Islam

Acceptance for the Council:
Anne Mayhew
Vice Provost and Dean of
Graduate Studies

(Original signatures are on file with official student records.)

A SIMULATION MODEL FOR THE FOUR PHASE SWITCHED-RELUCTANCE MOTOR

A Thesis
Presented for the
Master of Science
Degree
The University of Tennessee, Knoxville

James Thomas Cox III
May 2003

DEDICATION

This thesis is dedicated to the memory of my parents, James Thomas Cox Jr. and Bobbie Christine Walker Cox, who inspired me with their work ethic and encouraged me with their love, and to my wife and children whose love and support have been my rock.

ACKNOWLEDGMENTS

I wish to thank all those who helped me in completing my degree. I thank Dr. Lawler for his guidance throughout the process of writing my thesis. I thank all the professors who have contributed to my education at the University of Tennessee. They have demanded excellence and made me a better engineer. I especially thank Dr. Lawler, Dr. Crilly and Dr. Islam for serving on my committee.

I thank members of management at BWXT-Y12 who have supported and encouraged me while I was pursuing my degree. In particular, I would like to thank Andrea Zava whose words of encouragement have been a source of inspiration to me throughout my professional and educational career. I thank Philip Moor for his flexibility, support and understanding during the time this thesis was being written. Finally, I would like to thank J. Michael Cruse, who inspired me to finish my undergraduate degree and mentored me during that process.

ABSTRACT

The switched reluctance motor has become the topic of much discussion and research in the past few years. While it is one of the oldest motor types in existence, it has not made a big impact in industry, but because of its rugged and robust design, it has recently been viewed as a good candidate to replace other motor types as a workhorse for numerous applications. Notably among them are the traction applications such as vehicle drive. It is economical to manufacture and it is very rugged because of its simple construction. It is robust in that it is fault tolerant. A failure of one phase does not disable the motor completely. Unfortunately, it also has some drawbacks. Its design inherently produces torque ripple, an undesirable quality for vehicle applications, especially at low speed. This creates the need for more sophisticated means of controlling the motor.

This thesis describes a computer model by which the motor could be simulated and studied. The model is for a four phase switched reluctance motor and is written in MATLAB. It is hoped that this model could be used to research various control schemes, one or more of which could be used to make the switched reluctance motor a viable means of powering an electric vehicle.

TABLE OF CONTENTS

Chapter Page

LIST OF FIGURES

CHAPTER I
INTRODUCTION

In recent years, various types of electric motors have been investigated for use in traction applications. Several have shown promise, but also have drawbacks. The need for a motor that can be manufactured inexpensively and yet be rugged and reliable is evident in the automobile industry. The switched reluctance motor, which was originally conceived in the early 1800's [3], may be one that can fill that need.

Recently, the switched reluctance motor has gained considerable attention. It has the advantages of being inexpensive and rugged. Its simple construction makes it easy to manufacture but rugged enough to be worthy of consideration for powering traction applications such as automobiles [1]. But, it also has its drawbacks. The switched reluctance motor is inherently subject to torque ripple and acoustic noise [2]. This makes a more complex means of control necessary. Until recently, it was not considered a viable candidate for traction applications, but with improved methods of control it may be possible to design a method which would allow the use of the reluctance motor where smoother torque is required. Research into this application requires computer simulation and so a computer model is required. This work details one such model for the reluctance motor. The model was created in MATLAB and the code is included as an appendix.

The main objective of this thesis was to create an accurate and computationally efficient 4-phase SRM simulator to investigate SRM operation in low and high-speed applications. Secondly, we will explore the effects of varying the switching angles on power production with a particular interest in high speed, continuous conduction operation in one example of the use of this simulator. Finally, the

accuracy and efficiency will be demonstrated by comparing results of simulating with adaptive time steps and with a fixed time step.

In chapter two we begin with a mathematical analysis of the SRM with illustrations to explain the basic operation. Chapter three explains the model and the algorithms used in the simulation. Chapter four shows the simulation results with an emphasis on high-speed operation at continuous conduction. Chapter five lists the conclusions and the aims of further research.

CHAPTER II
ANALYSIS OF THE SWITCHED RELUCTANCE MOTOR

The reluctance motor is one of the oldest types of electric motors, yet it has found only an incipient market. However, it has been given considerable attention in the last two decades due to its simple and rugged topology. It is hoped that, under the right method of control, this motor could replace some of the workhorses in industry. Because of its simple construction it is durable and easily repairable. It is considered to be robust because of its ability to run under failure conditions.

The reluctance motor considered in this thesis is the 4 phase switched reluctance motor or SRM. It is called the 8/6 SRM due to the eight stator poles and six rotor poles. The torque that is produced is due to the attraction of the stator magnetic field to the iron in the rotor since the rotor has no windings or magnetic field. The rotor poles are wound such that opposite poles are continuations of the same pole.

General Discussion

The switched reluctance motor (SRM) is a doubly salient motor with no rotor winding. The motor under consideration is called a four-phase, 8/6 switched reluctance motor, referring to its 8 stator poles and six rotor poles. A graphical representation is presented below as figure 1. In the SRM, opposite stator poles contain the same continuous winding and thus, phase A consists of A and A' and is a single winding. Torque in the SRM is developed as solenoidal force as opposed to the Lorentz force that drives most motors, where both the stator and rotor produce magnetic fields. As pointed out by Becerra and others [4], the torque in the SRM is due to the tendency of a magnetic circuit to align itself to the position of least reluctance.

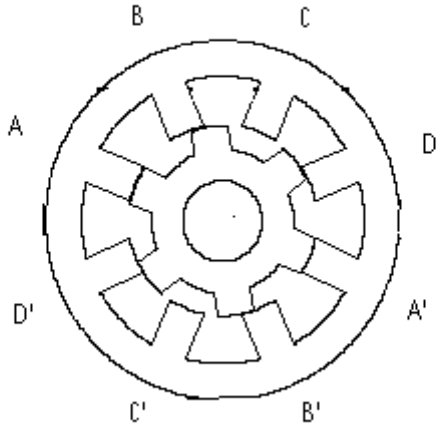

Figure 1 SRM Motor Schematic

Examination of figure 1 shows that the least reluctance will be realized when a rotor pole aligns with the energized stator pole. This configuration of phase A and the rotor poles is called full alignment and will be discussed later.
As will be seen, torque will be proportional to the derivative of the flux linkage of the energized pole.

A typical drive for the SRM is seen in figure 2. Motor winding A is energized when Q1 and Q2 are turned on. When Q1 and Q2 turn off, the motor winding will continue to conduct through D1 and D2 back to the power supply until the magnetic flux is discharged. Phases 2-4 will operate in a similar fashion with each successive phase causing the rotor to turn another step. The number of steps in a complete revolution and the step size are determined by the number of phases and the number of rotor poles as follows.

$$N_s = N_r \square P_s \qquad \text{(II.1.1)}$$

$$\theta_s = 2\pi / N_s \qquad \text{(II.1.2)}$$

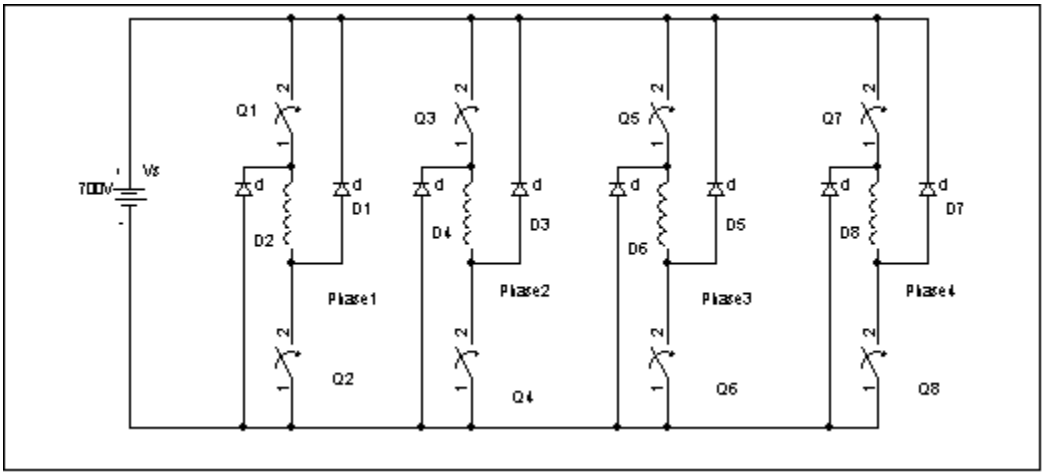

Figure 2 SRM Drive

In equations (II.1.1) and (II.1.2), Ns is the number of steps, Nr is the number of rotor poles, Ps is the number of phases and θs is the step size in radians. In the case of the four-phase, 8/6 SRM, the number of steps is 4*6 or 24. The size of the steps is 360/24 or 15 degrees. For a complete revolution of the rotor, each phase must be energized once for each of the six rotor poles. It can be seen from figure 2, that current through each of the phase windings is unidirectional. Torque is not dependent on the direction of current flow because there is only one magnetic field. This allows the use of a simpler motor drive.

As the rotor advances, a rotor pole will approach the next stator pole to be energized. The point where the leading edge of the rotor pole aligns with the stator pole's edge will be called θ_0. In the simulation model, which is discussed in the next chapter, this angle will define a reference point for energization of the stator pole. This is an arbitrary reference, which was chosen for convenience. This is the end of the unaligned position of the rotor and the beginning of alignment as illustrated in figure 3.

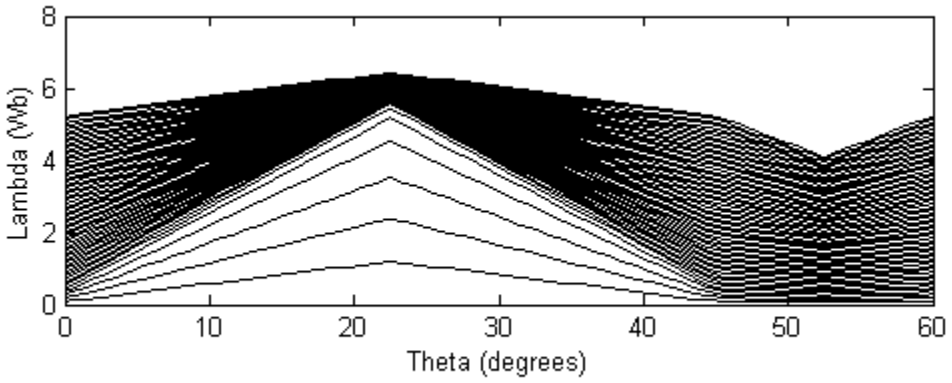

Figure 3 Lambda vs. Theta

Figure 3 shows zero degrees as the beginning of alignment. As the rotor continues to turn, there will be a greater degree of alignment and thus more inductance for the magnetic circuit because the magnetic path has less reluctance. Alignment and inductance will increase until the rotor pole is fully aligned with the stator pole A at 22 ½ degrees as in figure 3. Other angles of importance are the advance angle, θ_a, which defines the point at which the stator winding is energized, the commutation angle, θ_c, where power is disconnected from the phase winding, and the dwell angle, θd, which is the difference between θ_c and θ_a. Upon reaching the advance angle, the phase begins conducting though the transistor switches in the drive. At the commutation angle, when the transistors are cut off, the phase winding begins to discharge through the bypass diodes as shown in Figure 2. If the phase winding is conducting when the rotor passes from full alignment and the inductance begins to decrease, a braking torque will be developed.

Mathematical Analysis

The following discussion was derived from class notes by Lawler [5]. Each phase can be solved independently because of the weak coupling between phases. The operation of the phase winding can be described by the equation,

$$v = iR + \frac{\partial \lambda(\theta, i)}{dt} \qquad \text{(II.1.3)}$$

where v is the voltage applied to the phase winding by the inverter, I is the phase current, R is the resistance of the winding, λ, is the flux linkage, and θ, the position of the rotor. Equation (II.1.3) shows that λ is a function of both θ and the stator current.

The flux linkage curves for subject motor are shown in figures 3 and 4. These curves are plotted from discrete data points, which correspond to a motor model, which was developed by engineers at the Oak Ridge National Laboratory. Figure 4 shows the flux linkage plotted against current with rotor position used as a parameter. It can be seen that the flux linkage goes into saturation before the current reaches 100 Amperes where there is some degree of alignment. This makes the flux linkage more a function of rotor position but examination of the figure shows that current is still a factor.

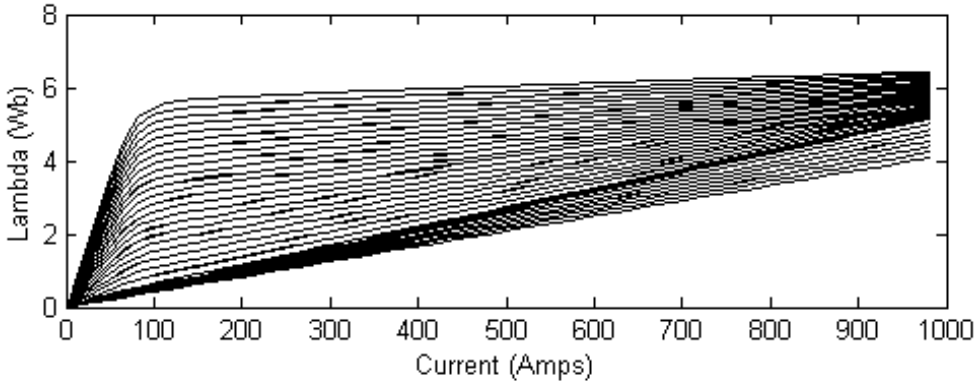

Figure 4 Lambda vs. Current

In figure 3, the flux linkage is plotted as a function of rotor position. Note that only 60 degrees of rotation are shown. This is all that is required because it is a periodic function. Figure 3 shows that in 60 degrees the flux linkage and inductance will rise and fall with rotor position. The onset of alignment, at zero degrees, corresponds to the leading edge of the rotor pole aligning with the edge of the incoming phase. For figure 3, one phase is shown and the others can be obtained by shifting the curves by 15, 30 and 45 degrees respectively. Recall that six cycles of this period are required for a complete revolution of the rotor.

Figure 5 illustrates the advance angle, which is point at which a winding is switched on, the commutation angle, where the winding is switched off, and the dwell angle, which is the total angle over which the winding is connected to the voltage source. The winding will continue to conduct after reaching the commutation angle until the inductor is discharged.

Equation (II.1.3) defined the relationship between the applied voltage, the current and resistance, and the flux linkage of the magnetic circuit.

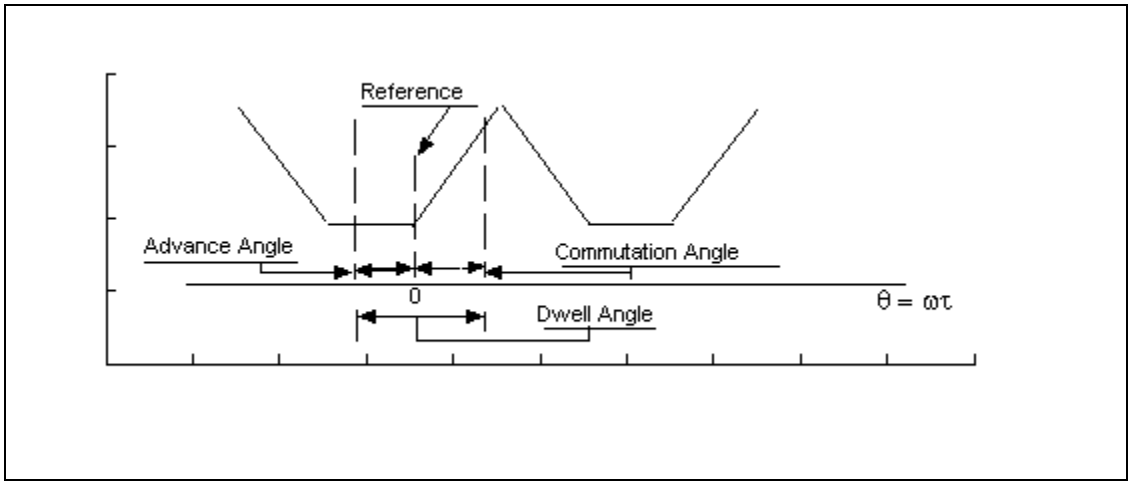

Figure 5 Angles Defined

Also, it was shown that the flux linkage is a function of the position of the rotor and the current flowing in the winding. This equation can be rewritten as

$$\begin{aligned} v &= ir + \frac{\partial \lambda(\theta, i)}{\partial i} \frac{di}{dt} + \frac{\partial \lambda(\theta, i)}{\partial \theta} \frac{d\theta}{dt} \\ v &= ir + \frac{\partial \lambda(\theta, i)}{\partial i} \frac{di}{dt} + \frac{\partial \lambda(\theta, i)}{\partial \theta} \omega \\ v &= ir + l(\theta, i) \frac{di}{dt} + e(\theta, i, w) \end{aligned} \tag{II.1.4}$$

where ω is the speed of the rotor, $l(\theta, i)$ is the incremental inductance and $e(\theta, i, \omega)$ is the pseudo back-emf of the motor. It is called pseudo back-emf because not all of the power, $ie(\theta, i, w)$, will provide mechanical torque for the motor. Some of this energy is stored as magnetic flux and returned to the power supply when the winding is de-energized. This energy will have a zero average value. In order to find the average power converted to torque, we will rewrite equation (II.1.3) as

$$\partial \lambda(\theta, i) = (v - iR)dt \tag{II.1.5}$$

Multiplying both sides of equation (II.1.5) by the phase current, integrating, and time averaging over a period of T we find the average mechanical power. This is given below in equation (II.1.6). First we find the power in a single phase and then extend that to include all four phases. This is the basis for one of the simulation equations and will be discussed in chapters three and four. T is the averaging period which corresponds to the angle over which we average and is equal to 60 degrees.

$$P_{phase=}\frac{1}{T}\int_0^T i(v-ir)dt$$

$$P_{phase=}\frac{1}{T}\int_{\lambda(0)}^{\lambda(T)} id\lambda \qquad \text{(II.1.6)}$$

$$P_m=\frac{4}{T}\int_{\lambda(0)}^{\lambda(T)} id\lambda$$

The last equation in (II.1.6) is the total average power for the motor. The appropriate interval for averaging would correspond, as before, to 60 degrees or $\pi/3$. Inserting this into equation (II.1.6) we have

$$P_m=\omega\frac{12}{\pi}\int_{\lambda(0)}^{\lambda(\frac{\pi}{3\omega})} id\lambda \qquad \text{(II.1.7)}$$

The torque is found by

$$T_m=\frac{P_m}{\omega}=\frac{12}{\pi}\int_{\lambda(0)}^{\lambda(\frac{\pi}{3\omega})} id\lambda \qquad \text{(II.1.8)}$$

A concept called co-energy is illustrated in the last equations. Co-energy is described by Sen [6] when discussing energy associated with the rotation of a motor. Figure 6 illustrates this concept. The area marked A in figure 6 represents the energy that is stored in the magnetic field around the phase winding. The area marked B in the figure is called the co-energy. While Sen maintains that it has no physical significance it can be used to calculate the torque and the torque producing power developed in a motor.

The flux linkage versus current plot, in which the co-energy integral exists, has traditionally been used to analyze the switched reluctance motor. [7]

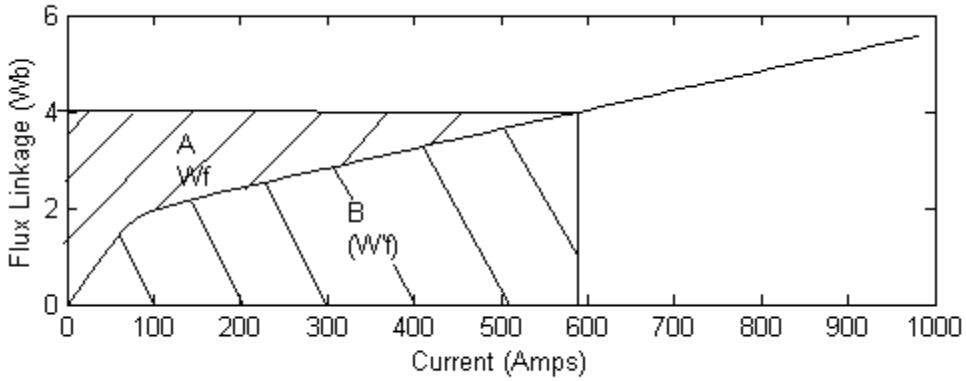

Figure 6 Typical Co-energy Plot

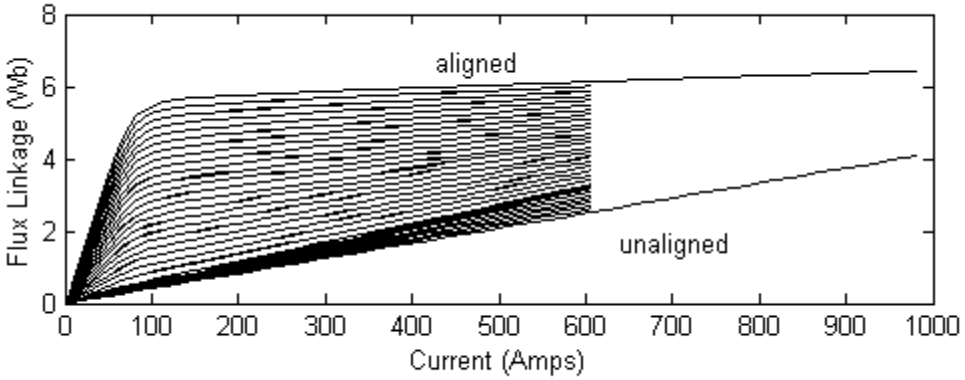

Figure 7 Co-Energy in the SRM

The co-energy for the SRM is equivalent to the integral in equation (II.1.8). This is illustrated above in figure 7. Figure 7 shows the co-energy as the shaded portion of the graph between the aligned and unaligned position of the rotor. It is plotted out to approximately 600 amps and shows the potential or maximum co-energy for this motor. In Miller's discussion of co-energy [3], he illustrates the effect of operating in saturation on the magnitude of the co-energy. Here he points out that operating in this region increases the ratio of co-energy to energy returned to the power supply, thus improving the efficiency of the motor.

Equation (II.1.4) indicates a first order differential equation that must be solved for each phase. We will repeat the conclusion to equation (II.1.4).

$$v = ir + l(\theta, i)\frac{di}{dt} + e(\theta, i, \omega) \qquad \text{(II.1.9)}$$

From equation (II.1.9), we see that the partial derivatives of the stator winding flux linkage will be required in order to simulate motor performance for this approach. The partial derivatives of the flux linkages for the example motor are shown in figures 8 and 9. Figure 8 shows the derivative of the flux linkage with respect to current and Figure 9 shows the derivative of the linkage with respect to rotor position. Note in figure 8 that the flux linkage starts out with a relatively sharp slope for most of the curves, and then tapers off to a much lower slope after reaching saturation at less than 100 amperes for higher levels of flux linkage. Figure 9 shows a constant slope for the flux linkage over most of the rotational period. This first 45 degrees corresponds to rotor positions that start out with the rotor and stator pole being point to point. This is the beginning of alignment. When the rotor reaches 22½ degrees it is at the fully aligned position and the sign of the derivative reverses. It continues at a constant negative slope until the rotor reaches 45 degrees and the rotor and stator poles are unaligned.

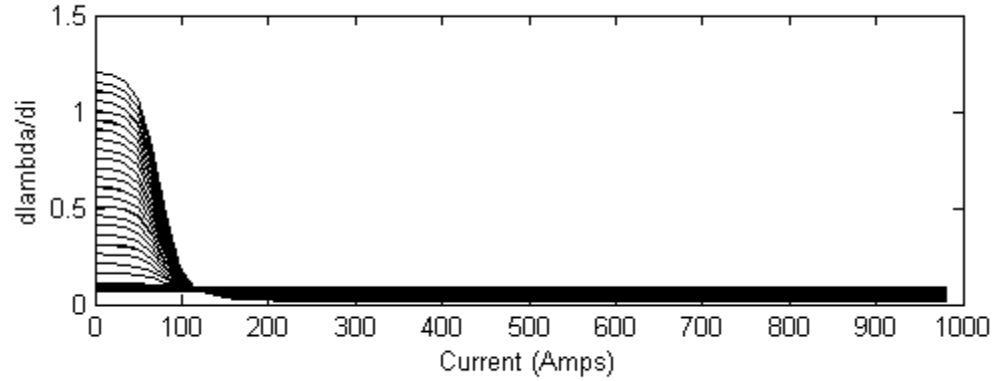

Figure 8 Partial Derivative of Flux Linkage with respect to Current

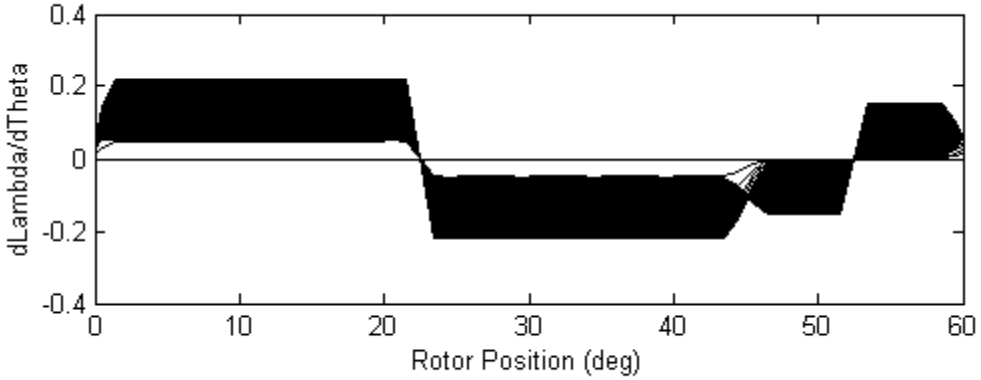

Figure 9 Partial Derivative of Flux Linkage with respect to Rotor Position

If current flows from 22 ½ degrees to 45 degrees, a braking torque will result. It is important to keep current levels to a minimum during this period.

The data for these figures was taken from the Oak Ridge National Laboratory (ORNL) flux linkage model that is being used in this study. In figure 8, rotor position was a parameter and in figure 9, stator current was a parameter. Other important aspects of motor operation include motor current and back emf. The solution to equation (II.1.9) is dependent on knowing the current. As we shall see in the development of the simulation, some difficulties arose in finding the current accurately, in particular, where an event occurs in which the current reaches a point where the regulator acts, or when the current reaches zero.

CHAPTER III
SIMULATION MODEL FOR THE SWITCHED RELUCTANCE MOTOR

General Discussion

Because of the difficulties in the analysis of the SRM, a computer simulation is required [8]. A simulation model based on static magnetization curves of the SRM is presented here.

The program is a general simulation of the SRM, written in Matlab, which could use any motor model. We have used a model designed by engineers at the Oak Ridge National Laboratory. The motor model becomes an input matrix to the program, called lam, and is a magnetic representation of the motor with data points in a matrix. Each row of the model represents a different phase winding current and each column corresponds to a different rotor position. Each data point represents the flux linkage at a specific current and rotor position. The data is used for two different ways of calculating operating parameters for the motor. First, the data is used as a look up table for finding the flux linkage at a given current and rotor position. Current is controlled by a hysteresis loop for both methods. In the first method, the data is interpolated for smaller steps, to give a closer approximation of actual motor performance. The second method calculates differential flux linkage from values of current, voltage and differential time, as we will show in the next section.

The program has three main sections. The first initializes parameters used in the program and sets the rotor to a specific position to begin rotation. The starting angle for this simulation was set arbitrarily to 45 degrees with theta being tracked relative to rotor position and coincident with phase B. The model simulates operation from 0 to 60 degrees of rotation because that is all that is needed to show operation of the motor. The second section is the main loop and it will

calculate flux linkage, current, back emf and power for each phase. The third section completes final calculations. Flux linkage, calculated in two different ways, is found in the output matrix, lamb, and will be a basis for comparison of the two methods. This model assumes adjustable, but fixed shaft speeds and does not contain dynamics for starting, changing speed, or load.

Each phase begins conduction 15 degrees after the previous phase begins and operation of each of the four phases is represented in 60 degrees. The period of conduction for each phase was initially set to begin at 0 degrees and end at 22 degrees relative to each phase respectively, but absolute rotor rotation is tracked as theta and is matched to the angular orientation of phase B. The zero degree position of theta corresponds to the beginning of alignment, or point to point position, for phase B. Because each rotor and stator pole is 22 ½ degrees wide, the initial setting for conduction begins at the point to point position and ends ½ degree before full alignment. Later we will explore the effects of varying this conduction period. With conduction set for 22 degrees and phases beginning conduction 15 degrees apart, there will be a 7-degree overlap period where two phases will be in conduction simultaneously. As stated previously, the flux linkage is calculated using two different methods. The first method is at the beginning of the main loop and is a look up and interpolation method. The rotor position angle is initially at 45 degrees, which is also 45 degrees relative to phase B. A vector has been initialized, threl, which contains the position angle relative to each phase. The angles in this vector begin 15 degrees apart and are defined relative to absolute rotor position, theta. Current levels are obtained from the vector, set, which is an input to the program. Set is initially established at 400 amps with a hysteresis band of 50 amps. The hysteresis is controlled by if/then statements, which modifies the value of the time change for a step of the main loop. The time for a step, dt, along with the rate of change of current is used to calculate new values of current, and flux linkage. Other inputs to the program include a vector of current values, cur, and rotor positions, rpos, which

correspond to the flux linkage data points in the input matrix, lam. The second method involves calculation derived from equation (II.1.5) using the following equation:

$$\lambda(t) = (v_a - i_a r)dt + \lambda(t - dt) \qquad \text{(III.1.1)}$$

where λ is the flux linkage, va is the winding voltage for phase a, ia is the winding current and r is the winding resistance. The first term on the right side of the equation is $\partial\lambda$, and the second term is the previous value of lambda. This statement is in a loop where all four phases will be calculated for their respective values on that particular step.

The flux linkage, or Lambda, is used to calculate instantaneous and average power. The following equation is employed.

$$E_{inst} = i_s d\lambda = i_s v dt \qquad \text{(III.1.2)}$$

where E_{inst} is the instantaneous energy or work, i_s is the instantaneous stator current and vdt is the voltage and differential time. Energy is accumulated for each step, then time elapsed is divided out to yield power. From the power we can also find the torque.

Chapter IV
SIMULATION RESULTS

Base Speed/Discontinuous Conduction

This program was simulated under the initial conditions of base speed of 288 RPM and discontinuous conduction and then under conditions of extended speed and advance angle and dwell. First we shall discuss the results of simulating under the initial conditions of zero starting angle and 22 degrees dwell, or duration of conduction. Because current flows for a period of time and then falls to zero, we call this discontinuous conduction. Figure 10 compares the results of the two different methods of calculating the flux linkage. The first part of figure 10 shows the results of calculating by accumulating or integrating successive values of voltage across the stator coil, and the second part displays the results of the look up and interpolation method.

In figure 10, the flux linkage is plotted against program steps for all four phases. Comparison of the first and second parts of the figure shows close correlation of the two methods. The second plot shows that the second method yield a slightly smaller value for maximum flux linkage, however, simulation with a greater number of program steps for the single rotation of the motor shows a tendency for convergence of the values. The graph is shown for 4000 program steps, but approximately 16,000 steps yielded a much closer convergence of the two methods. Because the look up method pulled its values from the model, this is the value we are trying to duplicate with the calculation method. Reduction of the number of program steps required for accurate reproduction of the model will be a goal of future study. A comparison of results from simulation runs using 16,000 and 4000 steps is shown in figure 11.

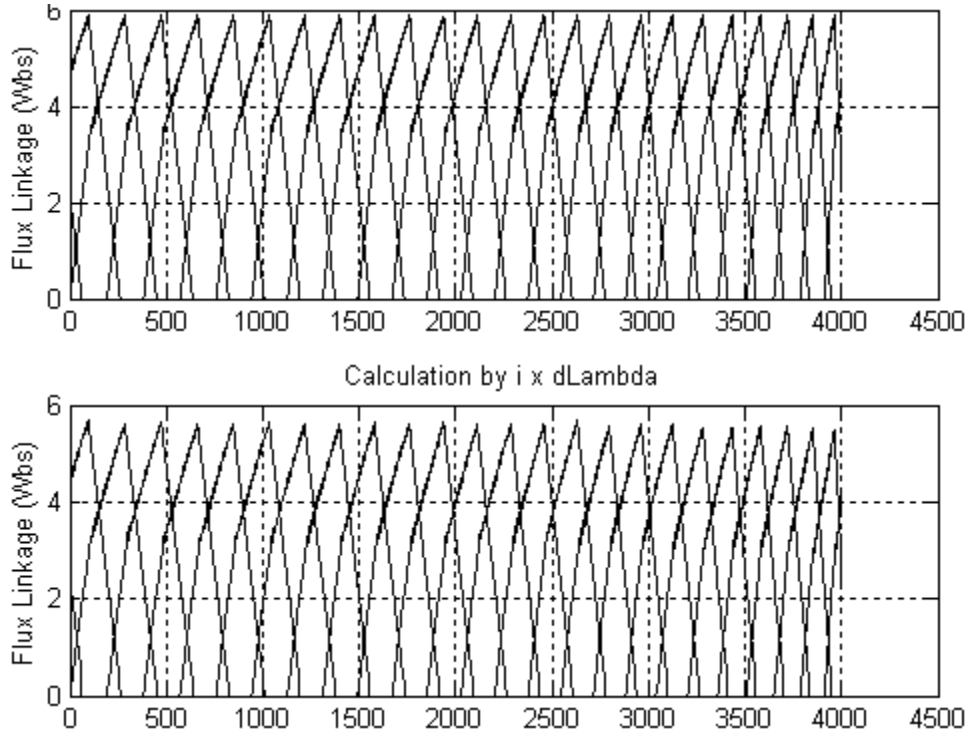

Figure 10 Comparison of Lookup and Calculation Methods

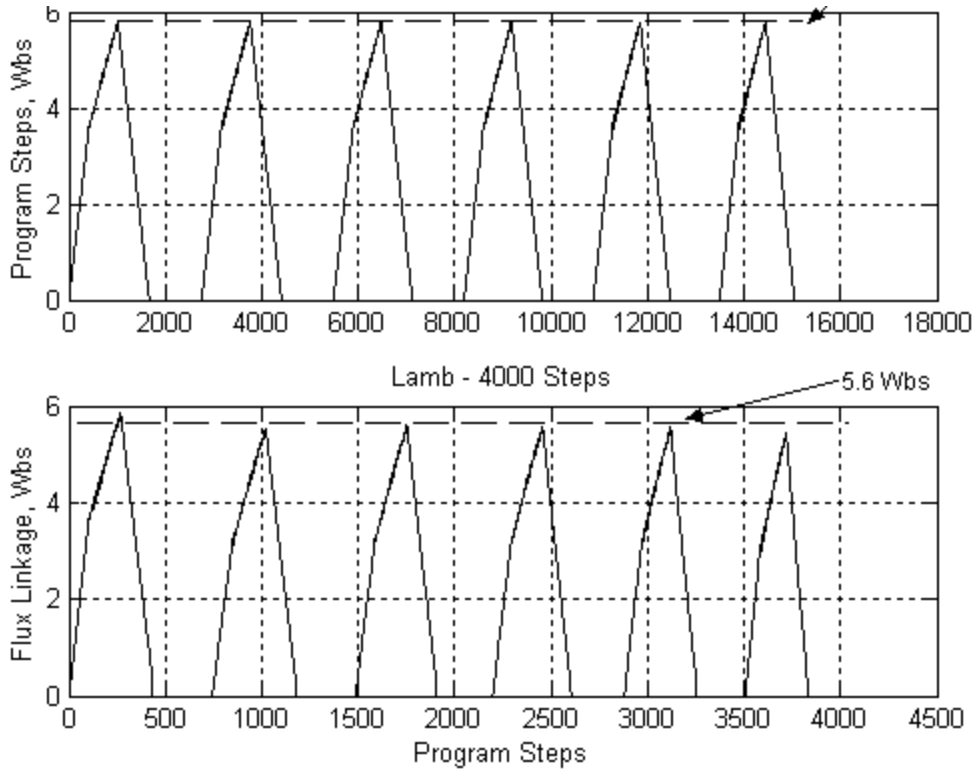

Figure 11 Flux Linkage vs Current for Lookup and Calculation Methods

In figure 12, are the current waveforms, plotted against program steps, for all four phases. The hysteresis or current regulation levels at the top of each current plot, were determined by the value of the input parameter, set, and were initialized to operate at 400A, with regulation points at 375A and 425A. The current regulation points presented one of the challenges for accurate simulation of this model. If the differential time, dt, is set to a constant value, the current levels may overshoot the certain critical points. These are illustrated in figure 13. The timing is critical at each of these five points. The critical events are the instant when current begins to rise from zero in response to a phase being switched on, any point when maximum current is reached and the regulator acts to limit current, any point when current reaches the lower regulation level, the point when the commutation angle is reached and the point when current again falls to zero. A section of code was written to check for overshoot and correct dt to bring the current just to the proper level. Differential time is first set to a constant, based on the speed of rotation, the number of program steps and the number of rotations being simulated. When an event in which one of the phases misses a regulation point occurs, dt is corrected to a value that causes that phase to just reach that critical value. Similar adjustments are made for rotor angle critical points, which are the advance angle and the commutation angle. For example, if we initially set the advance angle to 0 and the commutation angle to 22, it is desirable to have the simulation calculate current, flux linkage, and all the other parameters exactly at those angles. Figure 13 illustrates that the adaptive differential time scheme has accomplished that. At the initial angle, critical point one in figure 13, the current begins to increase until it reaches the current regulation point, in this case 400 amps. At critical point 4 in the figure, the rotor has reached the commutation angle and begins to decrease. With a constant time step, these critical points may have been missed and the accuracy of the simulation would have been lost. Because most parameters are calculated by adding a differential value to the previous value, all of the simulation would be affected.

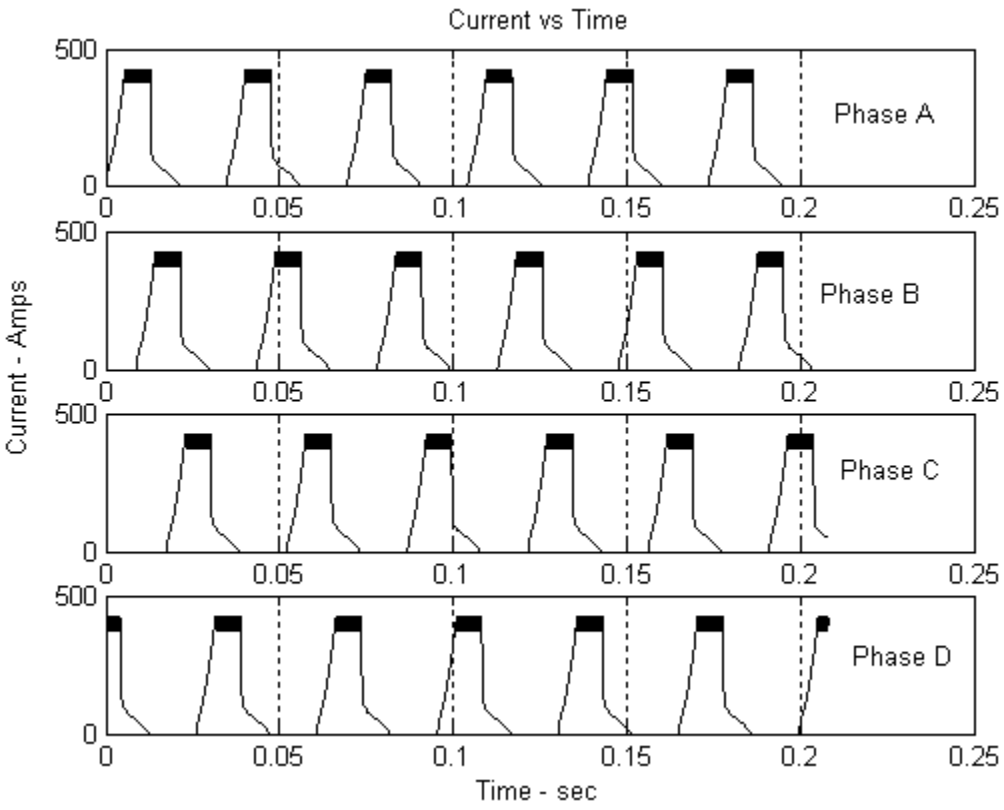

Figure 12 Four Phase Current Plot

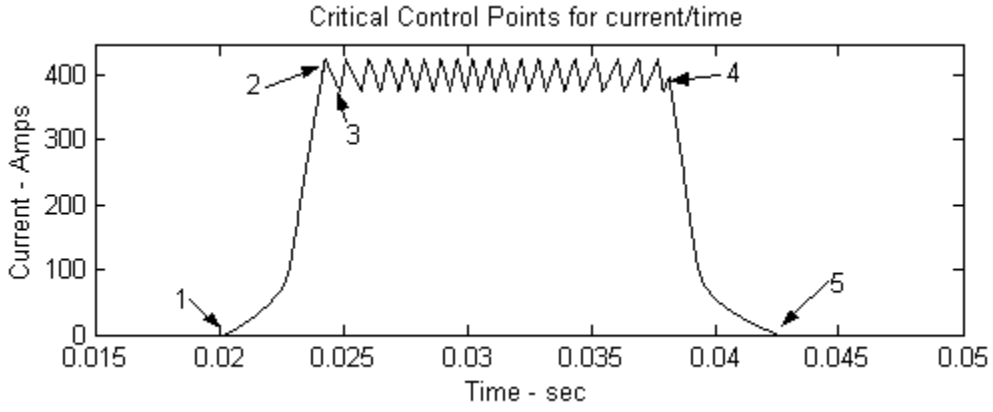

Figure 13 Critical Points in Time

One of the objectives of this thesis was to create an accurate and computationally efficient simulator for the SRM. The adaptive time step described in previous text helps satisfy that objective. Two tables have been prepared to illustrate the effects of adaptive differential time steps. Table one contains data taken from running the simulator without the adaptive time step. Instead, a constant time step is used and critical points are missed as a result.

From table one, we see that the current over shoots the regulation point of 400 amps, and overshoots the zero current level and records negative currents. Power supply diodes would cut the current off in an actual SRM, and therefore the negative current values are erroneous. At 6000 program steps, this simulation is finally hitting zero minimum current, but it is still overshooting the current regulation level at 16000 program steps. Also, RMS current levels are still a bit erratic at 16000 steps. Adjusting the time step to exactly step to each of these five points and the critical angles, results in the data contained in table 2. By comparison, the adaptive time step causes the calculations to converge more quickly and more accurately than a constant time step. Maximum and minimum current levels are met exactly with a minimum of steps when the adaptive time step is used. Accuracy in current calculations is essential to accurately calculating most of the other variables. Notable examples are flux linkage and power. RMS current in the adaptive case has converged to its final value of 206 amps at 3000 program steps.

It is clear from these tables that if a constant time step is used, accuracy and efficiency are sacrificed. The adaptive time step scheme is the key hitting the critical points and maintaining an accurate representation of SRM operation while keeping the model efficient by simulating in a minimum number of steps. The adaptive time scheme also improves with a greater number of steps, but much fewer are needed.

Table 1 Data Taken with Constant Time Steps

Number of steps	power Out	maximum current	minimum current	Irms
1000	3.9275 kW	484	-35	202
1250	3.6798 kW	485	-28	197
1500	3.7767 kW	459	-23	206
2000	3.6486 kW	464	-17	201
2500	3.5577 kW	451	-14	201
3000	3.5597 kW	453	-12	205
3500	3.5627 kW	448	-10	204
4000	3.5835 kW	444	-1	205
4500	3.5459 kW	436	-1	204
5000	3.5180 kW	441	-1	206
6000	3.5003 kW	434	0	205
8000	3.4677 kW	435	0	205
16000	3.4086 kW	429	0	206

Table 2 Data Taken with Adaptive Time Steps

Number of steps	power Out	maximum current	minimum current	Irms
1250	4.3416 kW	425	0	199
1500	4.0457 kW	425	0	204
2000	3.8515 kW	425	0	195 (204)
2500	37.845 kW	425	0	204
3000	36.693 kW	425	0	206
3500	3.6441 kW	425	0	206
4000	3.5711 kW	425	0	206
4500	3.6015 kW	425	0	206
5000	3.5613 kW	425	0	206

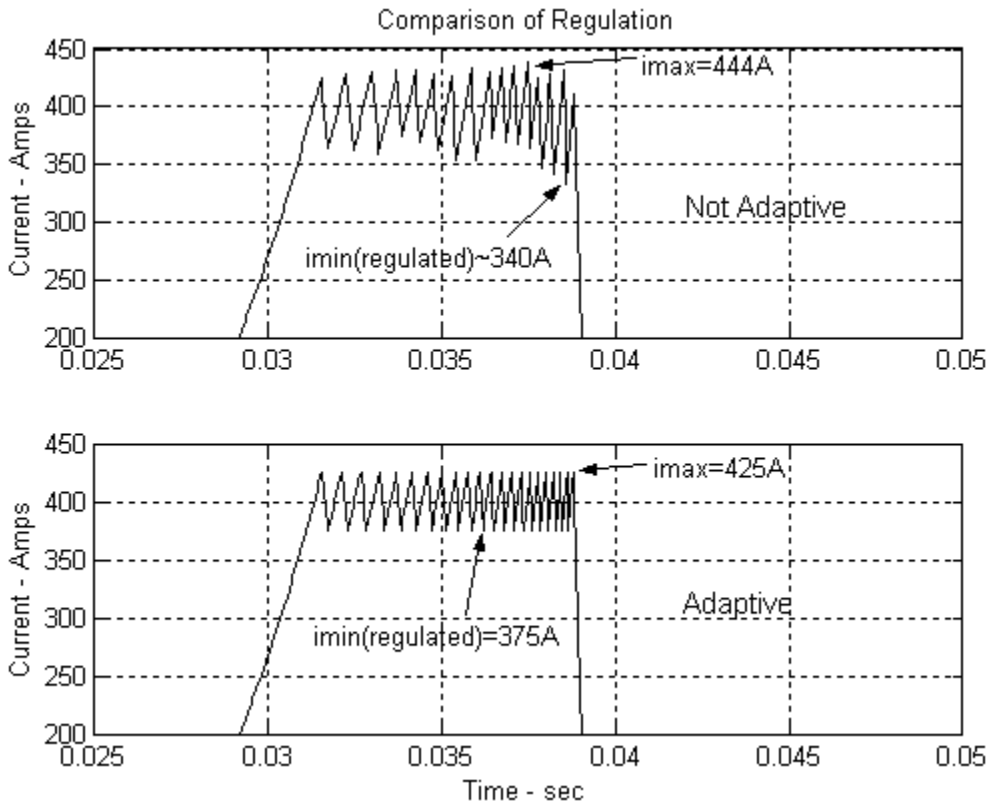

Figure 14 Comparison of Adaptive vs. Fixed Time Steps

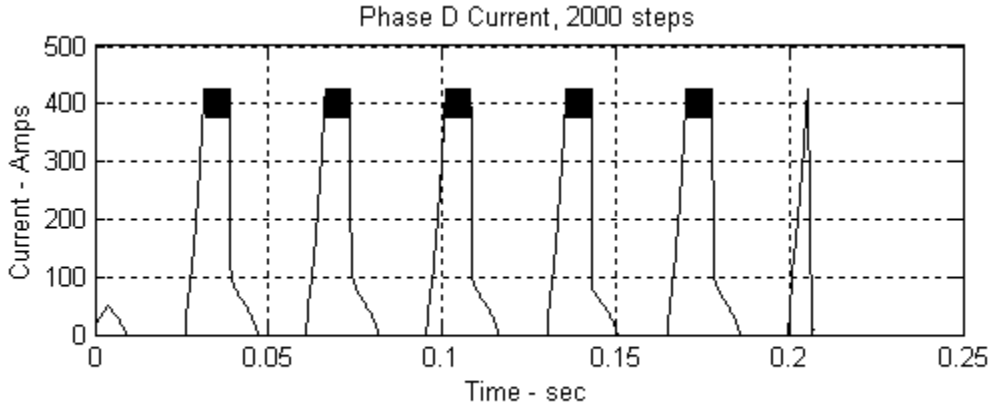

Figure 15 Anomaly in Current Plot with 2000 Steps

Comparison of adaptive and non-adaptive methods in figure 14 shows that the accuracy is greatly improved by the adaptive method. However, referring back to the table we see a discrepancy in the data for the case of 2000 program steps. The Irms current value in this entry is substantially different from those above it and below it in the table. This can be explained by figure 15. Figure 15 shows that on the last step of the program, phase D, which is the phase used for Irms in the table, drops to zero. Because the current is initialized to the last value of the current on the previous simulation, the current is at zero when the next simulation begins. By not reaching its full value, the current levels of the 60-degree cycle for phase D affects the calculation of the final value of RMS current. At the time of printing, the cause of this anomaly is unknown.

When the phase current passes through a winding, it generates a magnetic field, which in turn produces an EMF counter to the applied voltage. This back EMF is represented in figure 16 for a single phase. The other three phases were omitted for clarity. The back EMF is proportional to the rate of change of flux linkage with respect to a change rotor position and the rotor speed. The relationship is stated below in equation (IV.1.1).

$$e = \omega d\lambda / d\theta \qquad \text{(IV.1.1)}$$

In equation (IV.1.1), e is the back emf, ω is the radian rotor speed, and $d\lambda / d\theta$ is the rate of change of flux linkage with respect to position. The back emf is important in calculating power and torque in motors in general, but in this case, the back emf is called a pseudo back-emf, because it represents both energy that is used in torque production, and energy that returns to the power supply when the magnetic field collapses. Figure 16 depicts how the back emf responds during the rotation of the motor.

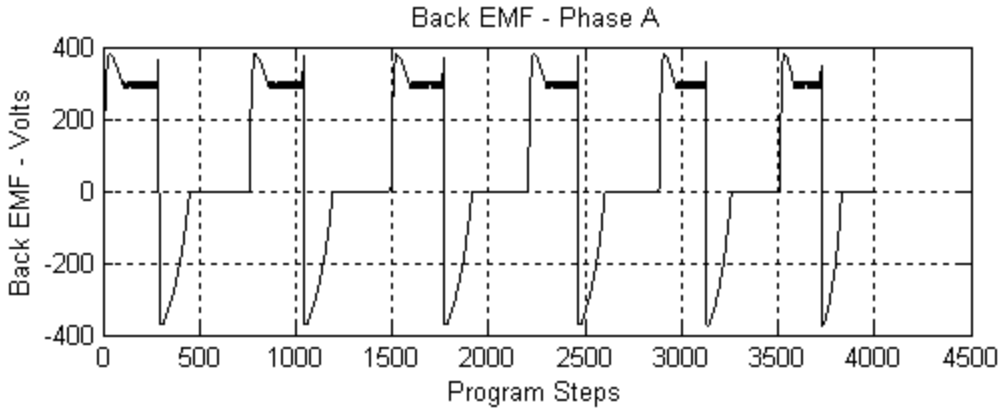

Figure 16 Back EMF

As the rotor comes point to point with the stator, flux linkage begins to increase at a relatively constant rate, thus creating the rippled, flat portion of the waveform at the top. The ripple reveals that flux linkage is also dependent on the current, which is being controlled within the hysteresis band. When the power supply is switched off and disconnected from the winding, the inductor discharges through the bypass diodes in the power supply and the sign of voltage on the winding is reversed. During periods of zero conduction, the back-emf, and the flux linkage itself, also go to zero. The pseudo back-emf presents opportunities for further study in showing a relationship between it and torque production.

Torque and power production in the switched reluctance motor is proportional to the co-energy, which was discussed earlier. In figure 17 is found the basis for calculating the co-energy, and thus the power and torque. In chapter II we stated that co-energy could be used for calculating the torque in a switched reluctance motor.

Figure 17 depicts flux linkage as a function of current. The familiar patter at the right of the figure is once again the current regulation area where the current level is maintained within the hysteresis band of 375A to 425A.

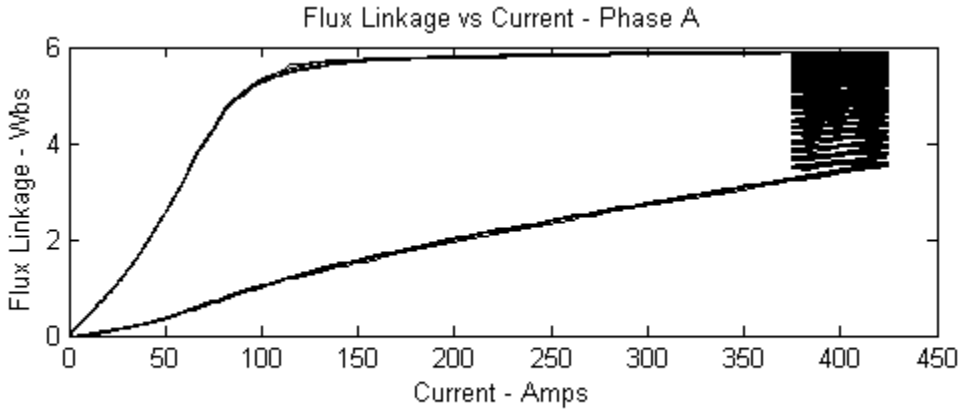

Figure 17 Flux Linkage vs. Current and Co-energy

Rotor position is a parameter in this plot and as we follow the flux linkage from zero along the bottom, up through the current regulation area and back along the top to zero, we are following the rotor position from zero, or point to point, to full alignment at the point of maximum flux linkage, then we see both the flux linkage and the current decrease to zero. If we integrate along this path from zero back to zero, we will find that the area represents the co-energy, which is proportional to torque and power. In the program we have integrated around this path by accumulating consecutive values of $id\lambda$ as illustrated in chapter II. We note the nearly linear nature of the bottom line in this figure that illustrates flux linkage as being nearly linearly proportional to current until saturation effects begin to appear. The top of the curve is the area where the power supply is switched off and the winding is discharging back through the bypass diodes. Referring back to figures 4 and 5 in chapter 2, we see that $d\lambda$ becomes negative when the rotor passes through the fully aligned position and the degree of alignment is decreasing. In this region, the differential flux linkage is negative, which generates a braking torque to the rotor and the machine now operates as a generator.

Saturation effects in this and other figures decrease the rate of increase of flux linkage, which is important for torque production. Further, increases in inductance decrease the rate of increase of current flow to the point where current flow actually begins to decrease. Therefore it is advantageous to have high current levels when the rotor reaches the beginning of alignment. Because of the braking torque generated when $d\lambda$ becomes negative, the winding should be de-energized when we reach the fully aligned position. This discussion will be picked up again later in this chapter as we investigate the effects of varying the conduction angles. This area of study has been a focus of personnel at the Oak Ridge National Laboratory in recent years and becomes the major purpose of this model.

Figure 18 below, illustrates the rate of change of flux linkage with respect to rotor position for the given current regulation level. The linear area is shown to occur for most of the 22-½ degrees the rotor travels from point to point position to fully aligned position. From 22 ½ degrees to near 34 degrees the flux linkage decreases back to zero, giving a negative value for $d\lambda$. For the remainder of the 60 degrees, the flux linkage and $d\lambda$ will be zero.

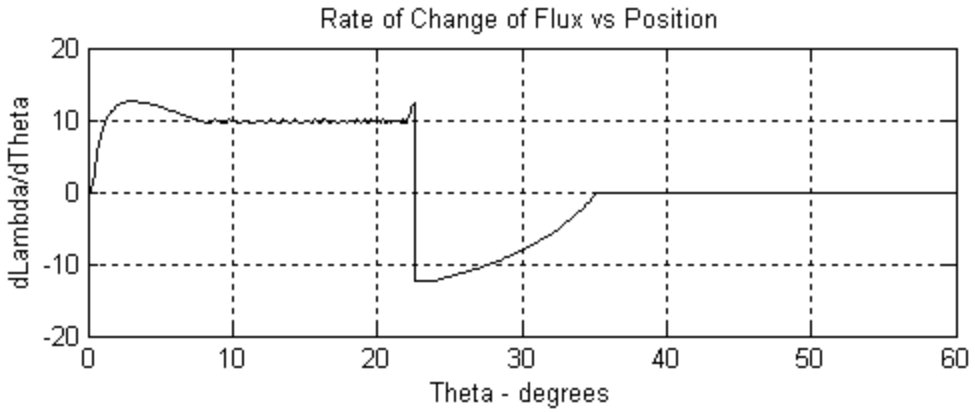

Figure 18 Rate of Change of Lambda vs. Theta

Figure 19 shows the rate of change of flux linkage with respect to current. The rate of change is quite small throughout the cycle. However, it should be noted that the flux does change with respect to changes in current and this effect must be accounted for in any analytical model. The rate of change is nearly flat during the period where the rotor progresses from point to point with the rotor to full alignment. This is a departure from the response of flux linkage in equation (IV.1.2)

$$\lambda = Li \tag{IV.1.2}$$

Equation (IV.1.2) indicates a direct correspondence of flux linkage to a change in current. The departure that we see in figure 19 is due to magnetic saturation. The iron in the rotor and stator cause the inductance to increase and the large current drives the flux linkage into saturation.

This non-linearity makes an analytical approach quite difficult and will require more research if a satisfactory analysis can be completed. This computer model takes into account any change in flux for any reason and this figure has been included as a point of interest.

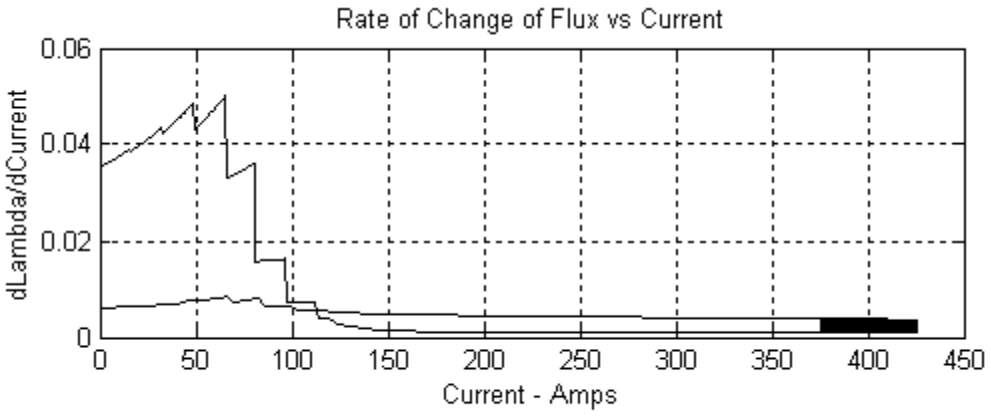

Figure 19 Rate of Change of Lambda vs. Current

Effects of Varying Conduction Angles

In the previous discussions we have considered the operation of the switched reluctance motor with a somewhat standard set of operating conditions, namely, we specified conduction angles to begin at zero and end at 22 ½ degrees. We have seen that these conduction angles are important from the standpoint that we would like for current to begin at a high level at the same time the rotor pole begins to increase the inductance of the magnetic circuit by becoming aligned with the stator pole. We would also like to end the conduction cycle early enough to avoid creating braking torque or operating as a generator. We now consider the effects of varying those stated conditions and running at greater than base speed.

Realizing that time elapses between closing the switch in the power supply and reaching full current, and desiring to be at full current when the inductance begins to increase, we shall explore the effects of beginning conduction some period of time before reaching zero degrees. By keeping the cut off angle the same, we also increase the period of conduction. In figure 20, plots are shown of the flux linkage with respect to current for two different advance angles. In a), an advance angle of zero is used, matching the conditions we have assumed thus far. In b), the advance angle becomes 5 degrees and the co-energy has increased. Causing the stator winding circuit to fire early allows current to build up in the winding before torque production begins and also before the rotor and stator enter the alignment period. It is in this area that the conduction can become large without saturating the iron in the rotor and stator. Because the inductance is low, the flux linkage will also be low and magnetic saturation is not an issue. We will explore this phenomenon more in following discussions. The effect of increasing the advance angle is to increase the available torque.

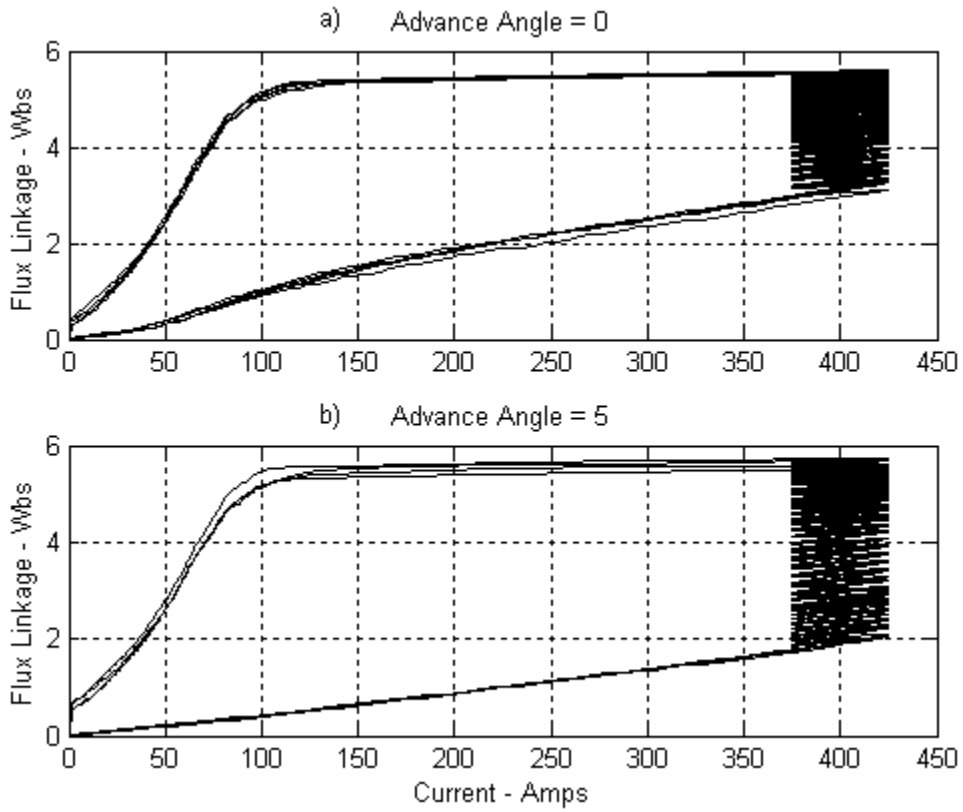

Figure 20 Co-energy Change due to Increased Advance Angle

We also note that the conduction angle was also increased by 5 degrees, shutting off the winding at the same commutation angle that we used before.

Next, we consider high-speed operation at weak continuous conduction. It is called weak conduction because the regulator is never required to act to limit the current. With an advance angle of 25 degrees and a dwell of 31 degrees, we see in figure 21 that the current does not reach the prescribed 600 Amps. Instead the current reaches a maximum of around 385 Amps. Minimum conduction levels are at 20 Amps. At 385 Amps the regulator is never required to limit the current and this is called weak continuous current. A plot of co-energy appears in Figure 22. This area is small in comparison with others we have shown, but it represents energy generated over a smaller period of time.

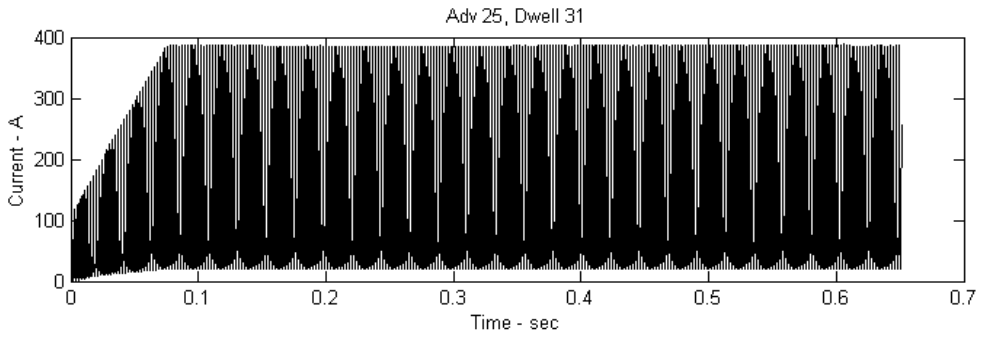

Figure 21 Current Levels and Buildup for Weak Continuous Conduction

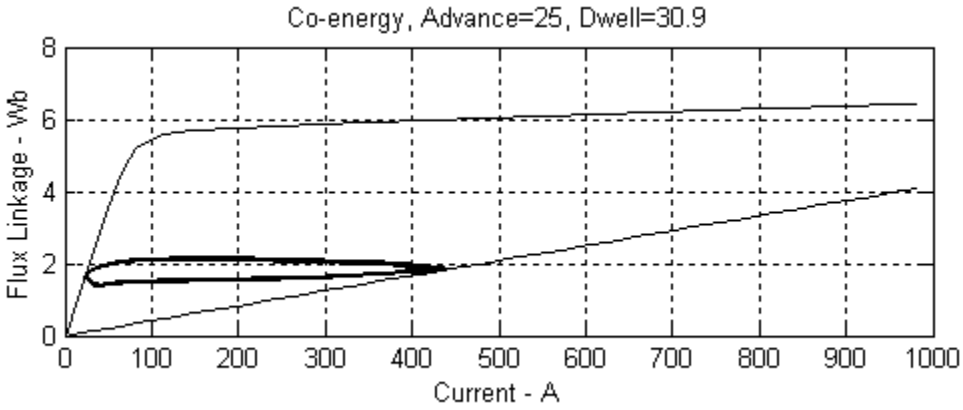

Figure 22 Co-energy under Weak Conduction

Figures 21 and 22 correspond to a speed of 16 times the base speed or 4608 RPM, and advance angle of 25 and a dwell of 30.9 degrees. The current has not reached the set value of 600, as we will see in figures 21 and 22, the co-energy is not reaching its potential.

In figure 23, with only a half-degree more advance angle, the regulator is required to limit the current to 625 Amps and regulate around 600 Amps. This is called strong continuous current. Minimum current during continuous conduction for this case is around 35 Amps. Figure 24 shows the co-energy plot for 31 degrees and it reveals a jump in energy from figure 22. When the difference is a full degree, this jump becomes quite pronounced. Lawler's experiments yielded similar results [5]. We will show in subsequent figures that a major bifurcation exists around this jump. It will be the subject of further study.

Another important observation to make from figure 24 is the fact that the machine has moved into linear operation. Comparing figure 24 with figure 20, we find that most of the conduction at high speed, constant current, takes place before the rotor begins to align with the stator. The winding is turned off and the current has fallen to zero before a significant degree of rotor-stator alignment takes place. Because the iron in the magnetic circuit is at a minimum, saturation effects associated with high current levels and magnetic flux in iron are eliminated. While it is not the purpose of this work to investigate linear operation of the SRM, this phenomenon could prove to be an important area of future research. Other types of motors are routinely operated without entering the magnetic saturation limitations of the iron. It may also be possible to operate the switched reluctance motor linearly during high speed operations, while producing power and torque levels that are comparable to the levels achieved in conventional motors. The SRM could become an important alternative to the expensive motors currently in use.

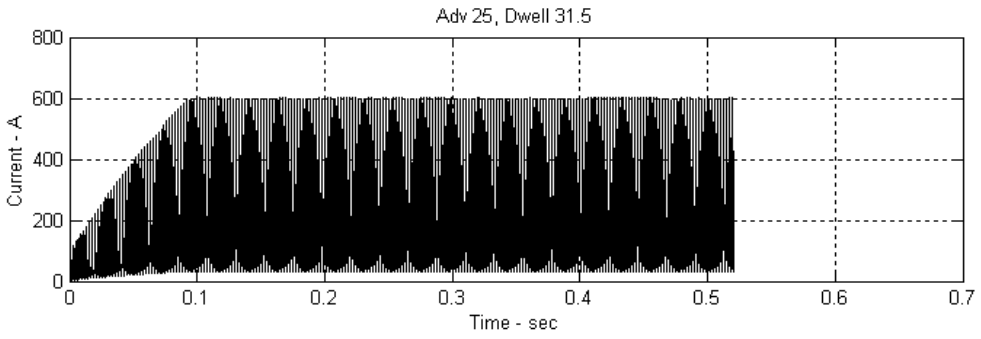

Figure 23 Current Levels and Buildup under Strong Continuous Conduction

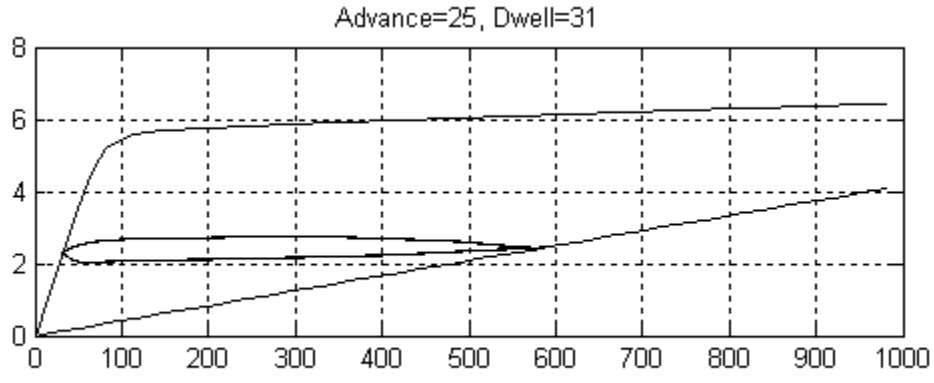

Figure 24 Co-energy under Strong Continuous Conduction

Lang and Vallese pointed out that for unsaturated operation, the flux linkage versus current curves are linear and that the slope of these lines is dependent on inductance, which is a function of rotor position [9]. For the strong continuous current case, most of the current conduction occurs while the rotor and stator are unaligned and inductance is nearly constant. Flux, then, becomes a function of current and a constant.

Another effect associated with constant current is the bifurcation mentioned previously. This effect is associated with the jump in energy we saw in the co-energy plots of figures 22 and 24. If the advance angle is increased, while the commutation angle is held constant, there is a point where the RMS current and the power production of the machine jump from a low level to a much higher level. This effect is illustrated in figure 25, where total machine power and RMS current are plotted against advance angle. The commutation angle is a parameter. Speed of rotation for this plot is set at 16 times base speed. The figure reveals that at the proper advance angle and dwell, power and current are dramatically larger than at lower advance angles and dwells. However, past the critical angle, the power begins to decrease. Figure 25 illustrates that it is possible to achieve high power outputs at speeds well beyond base speed. Figure 26 is added for comparison. Operating speed for the plot in figure 26 is four times the base speed. The same effect is evident in figure 26, but to a lesser degree. While the power increases by around 400 kW at 16 times base speed, the increase is only about 250 kW for 4 times base speed. With modern feedback and control methods, it should be quite possible to control the advance and commutation angles such that this power increase is sustainable at high speed and strong continuous current. This will also make the switched reluctance motor competitive with other motor types for power and torque production.

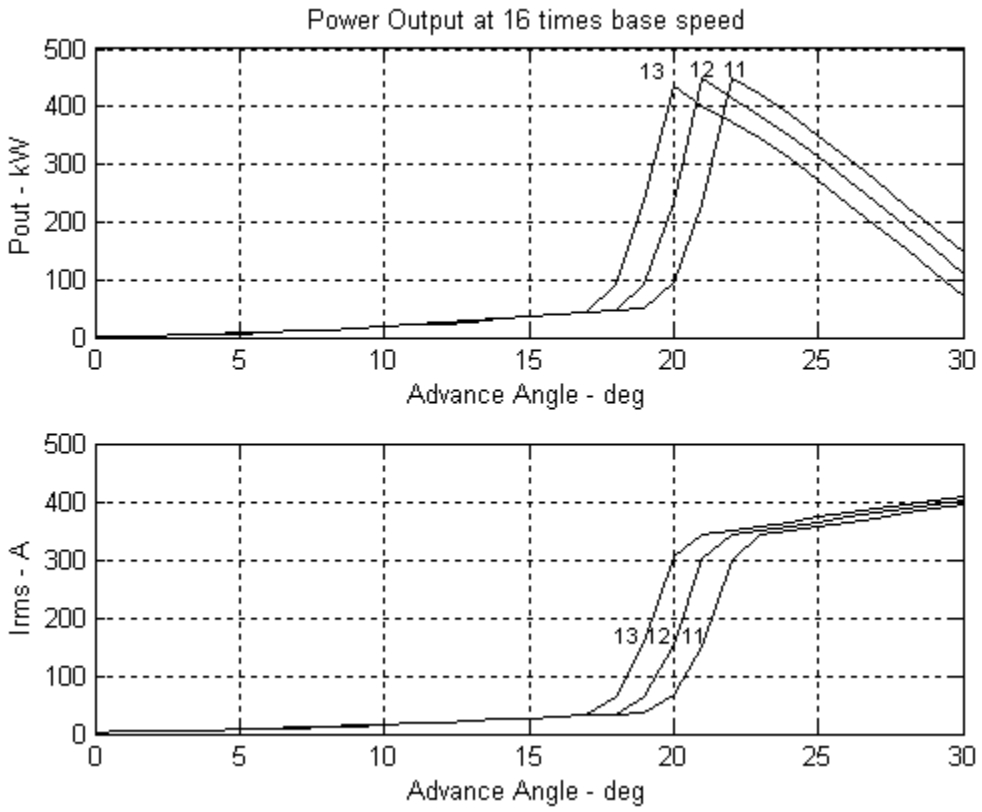

Figure 25 Bifurcation Plots for 16 Times Base Speed

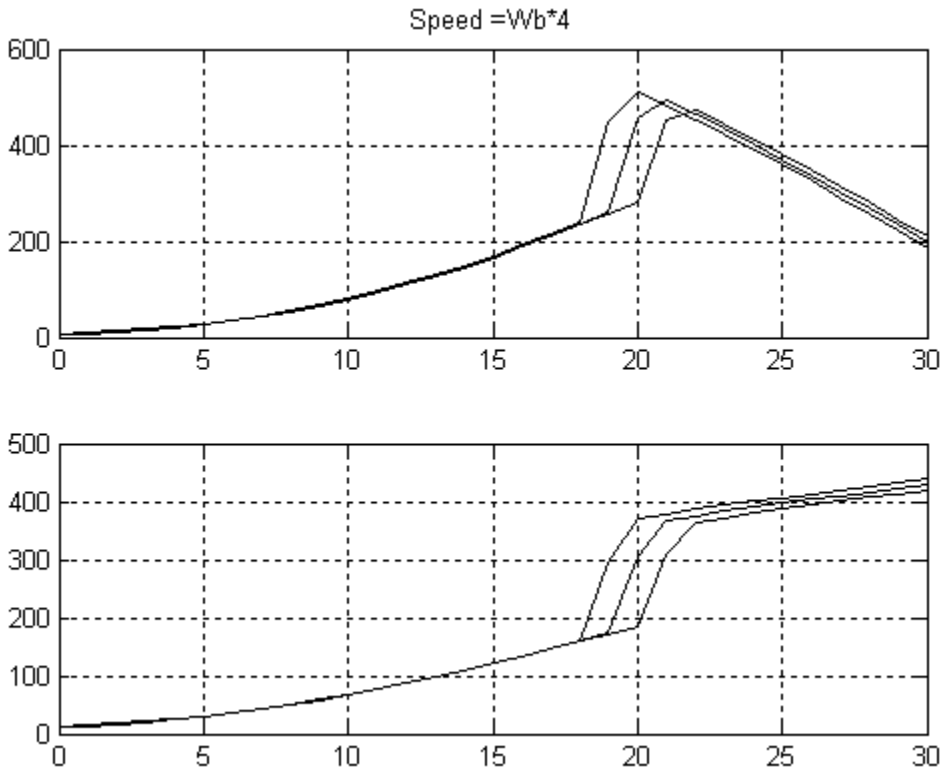

Figure 26 Bifurcation Plots for 4 Times Base Speed

CHAPTER IV
CONCLUSIONS

The Matlab model presented in this thesis can be used to simulate steady state operation of the switched reluctance motor. It differs from the usual single-phase model in that all four phases are represented. The flux waveforms are calculated and can be plotted by two different methods. A look up table of data points generated by engineers and the Oak Ridge National Laboratory is employed to provide a model for comparison. Flux linkage is then calculated using current and voltage. The comparison of the two methods is favorable, but requires many program steps for an accurate reproduction. One goal of further study would be to reduce the number of program steps required, thereby increasing the speed.

Power is calculated for the SRM from the look up model and from the calculated model. It has been pointed out by several authors that accurate instantaneous power would be difficult to calculate and that is the case with this model. Another goal of further research would be to find an algorithm that could accurately perform this function. Good estimates of average power can be obtained by using this model.

It was noted in the discussions that variation of the conduction angles, including the firing angle, produces interesting results. A bifurcation exists where power rises rapidly with an earlier firing angle, but falls off quickly when the size of this angle is excessive. Other authors have suggested a bias current for the windings to achieve continuous current, but this study shows that continuous current can be achieved by controlling the advance and commutation angles. In his lecture notes, Lawler [5] points out that due to the sharpness of the transition, the motor could slip out of high continuous conduction with a resulting decrease in speed. This problem could be avoided by temporarily increasing the commutation angle. Lawler further states that faster buildup to steady state can

be achieved by the same method. This would require an intelligent controller with feedback. This phenomenon could be the basis of future research into the use of the SRM for high power applications. In addition, the high speed study revealed that linear operation is possible with continuous high level current flow in the windings.

LIST OF REFERENCES

LIST OF REFERENCES

[1] Cheok AD, Fukuda Y : *A New Torque and Flux Control Method for Switched Reluctance Motor Drives,* IEEE Transactions on Power Electronics, Vol. 17, no. 4 July 2002

[2] Staton DA, Soong WL, Miller TJE : *Unified Theory of Torque Production in Switched Reluctance and Synchronous Reluctance Motors,* IEEE Transactions on Industrial Applications, Vol. 31, no. 2, March/April 1995.

[3] Miller TJE : *Brushless Permanent-Magnet and Reluctance Motor Drives,* Clarendon Press (Oxford), 1989

[4] Becerra RC, Ehsani M and Miller TJE : *Commutation of SR Motors.* IEEE Transactions on Power Electronics, Vol. 8, No. 3, July 1993.

[5] Lawler JS : ”Unpublished Lecture Notes on the Switched Reluctance Motor”

[6] Sen PC : *Principals of Electric Machines and Power Electronics,* John Wiley & Sons, 1989.

[7] Staton DA, Deodhar RP, Soong WL, Miller TJE : *Torque Prediction Using the Flux-MMF Diagram in AC, DC, and Reluctance Motors,* IEEE Transactions on Industry Applications, Vol. 32, no 1, January/February 1996.

[8] Miller TJE, McGilp M : *Nonlinear Theory of the Switched Reluctance Motor for Rapid Computer-Aided Design*, IEE Proceedings, Vol. 137, Pt. B, no. 6, November 1990.

[9] Lang JH, Vallese FJ : *Final Report: Variable Reluctance Motor Drives for Electric Vehicle Propulsion,* DOE/CS/54209-26 (DE85017585), Technical Information Center, Office of Scientific and Technical Information, United States Department of Energy.

APPENDIX

APPENDIX

Matlab Code Listing

```
function
[t,i,irms,e,pout,pavg,v,x0,ps,lamb,dldc,dlda,tconb,bifur,Irms]=srmtomMar3_24_2
        (cur,rpos,lam, vdc,p,n,nb,r,nsteps,set,advcon,nc,x0,deltai);
global dldi dldp pavgdc avgpout avgpout2 lam0 lam00 theta t i v lammax idc
avgidc poutinst swfac lamb2;
global va Swfac lamb iaold ianew x0 Threl bifur rms avg Dianew Irms
Swfac=[];
Dianew=[];
thresh=cur(2);
ncur=length(cur);
rpos=(p/2)*pi*rpos/180;  %
npos=length(rpos);       %
dldp=zeros(ncur,npos);
dldi=dldp;
lm=zeros(ncur-1,npos);
for k=2:ncur,
  lm(k-1,:)=lam(k,:)/cur(k);       % Calculates inductance, not used
end;                               % elsewhere
lmin=lam(10,54)/cur(10);
for k=1:npos-1,
  dldp(:,k)=(lam(:,k+1)-lam(:,k))/(rpos(k+1)-rpos(k));
end;
dldp(:,npos)=dldp(:,1);

for k=1:ncur-1,
  dldi(k,:)=(lam(k+1,:)-lam(k,:))/(cur(k+1)-cur(k));
end;
```

```
dldi(ncur,:)=dldi(ncur-1,:);
thon=advcon(1)*pi/180;                % Converts advcon to radians
thcond=advcon(2);
thcond=thcond*pi/180;
wb=(p/2)*2*pi*nb/60;w=n*wb;
ihi=set(1)+set(2)/2;ilo=set(1)-set(2)/2;
dth=2*pi/nsteps;dt=dth/w;dto2=dt/2;
dtt=dt;
nsteps=nc*nsteps;
period=nsteps*dt;
theta=zeros(nsteps+1,1);
%i=zeros(nsteps+1,4);
idc=zeros(nsteps+1,4);
%e=zeros(nsteps+1,4);
%pwr=zeros(nsteps+1,4);%
v=zeros(nsteps+1,4);
va=zeros(1,4);
t=zeros(nsteps,1);
%irms=zeros(nsteps+1,4);%
%pavg=zeros(nsteps+1,4);%
dldc=zeros(nsteps+1,4);
dlda=zeros(nsteps+1,4);
ps=zeros(nsteps+1,4);
lamb=zeros(nsteps,3,4);
lamb(1,3,:)=lam0;
lamb(1,1,:)=lam0;
pavgdc=zeros(nsteps+1,1);%
pout=zeros(nsteps+1,4);%
pout2=zeros(nsteps+1,4);%
poutinst=zeros(nsteps+1,4);%
```

```
accdcv=0;xx=0;%
delT=dt;
acclam=0;avgpout=zeros(1,4);avgpout2=zeros(1,4);swfac=[1 1 1 1];%
accidc=zeros(1,4);
adv=advcon(1)*pi/180;
rms=0;avg=zeros(1,4);
thh=0;th=pi/4;threl=[th+pi/12 th th-pi/12 th-pi/6];
for index = find(threl>pi/3)
    threl(index)=threl(index)-pi/3;
  end
  for index = find(threl<0)
    threl(index) = threl(index)+pi/3;
  end
kth=[1 1 1 1];
while th>rpos(kth(2)+1),
 kth(2)=kth(2)+1;
end;
for index = 1:4
  while threl(index)>rpos(kth(index)+1)
    kth(index)=kth(index)+1;
  end
end

ktt=kth;
thnext=rpos(kth(2)+1);
%thoff=thon+thcond;
%dianew = [0 0 0 0];
iaold=[x0(1) x0(2) x0(3) x0(4)];
diaold=[x0(5) x0(6) x0(7) x0(8)];%Set up iaold & diaold
kia = [kth(1) kth(2) kth(3) kth(4)];
```

```
for index = find(kia>61)
   kia(index)=kia(index)-60;
end
i=zeros(nsteps,4);
i(1,:)=iaold;
for index = 1:4
   if iaold(index)<=thresh,
      kc(index)=1;
   else
      kc(index)=fix((iaold(index)-thresh)/deltai)+2;
   end

   if kc(index)>=ncur-1,
      kc(index)=ncur-1;
   end
end;
kcc=kc;
%  Set thon/thoff
thon1 = 0-adv;
thoff1 = thon1+thcond;
thon1 = [thon1-pi/12 thon1 thon1+pi/12 thon1 + pi/6];
thoff1 = [thoff1 - pi/12 thoff1 thoff1 + pi/12 thoff1 + pi/6];
for index = find(thon1<0)
   thon1(index)=thon1(index)+pi/3;
end
for index = find(thon1 >= pi/3)
   thon1(index)=thon1(index)-pi/3;
end
```

```
for index =find(thoff1>=pi/3)
   thoff1(index) = thoff1(index)-pi/3;
end
for index = find(thoff1<0)
   thoff1(index) = thoff1(index)+pi/3;
end
% End Set thon/thoff

% Set op
global Dt Ianew;
Ianew=[];
Dt=[];
op=[];
thnew=th;
thold=th-dth;
tcon=0;
%lamb(1,1,:)=lamb(1,3,:);
%  Main Loop
global Fac1 Fac2;
%lamb(1,1,:)=lam0;
Threl=threl;
for k=1:nsteps,
   Threl=[Threl; threl];
   for index = 1:4
        fac1(index)=(threl(index)-rpos(kth(index)))/(rpos(kth(index)+1)-
        rpos(kth(index))); % fac1 is a 1x1 matrix
        fac2(index)=(iaold(index)-cur(kc(index))')/(cur(kc(index)+1)'-
        cur(kc(index))');   %fac2 is a 4x1 matrix
```

```
        dlc1(index)=(lam(kc(index),kth(index)+1)-
        lam(kc(index),kth(index)))*fac1(index)+lam(kc(index),kth(index));  % dlc1 is
        a 4x1 matrix
        dlc2(index)=(lam(kc(index)+1,kth(index)+1)-
lam(kc(index)+1,kth(index)))*fac1(index)+lam(kc(index)+1,kth(index));  %
        dldc(k+1,index)=((dlc2(index)-dlc1(index))/(cur(kc(index)+1)-
cur(kc(index))))';
        dla1(index)=(lam(kc(index)+1,kth(index))-
lam(kc(index),kth(index)))*fac2(index)+lam(kc(index),kth(index));
        dla2(index)=(lam(kc(index)+1,kth(index)+1)-
lam(kc(index),kth(index)+1))*fac2(index)+lam(kc(index),kth(index)+1);
        dlda(k+1,index)=(dla2(index)-dla1(index))/(rpos(kth(index)+1)-
rpos(kth(index)));
        lambda1(index)=(lam(kc(index),kth(index)+1)-
lam(kc(index),kth(index)))*fac1(index)+lam(kc(index),kth(index));
        lambda2(index)=(lam(kc(index)+1,kth(index)+1)-
lam(kc(index)+1,kth(index)))*fac1(index)+lam(kc(index)+1,kth(index));
        lamb(k+1,3,index)=(lambda2(index)-
lambda1(index))*fac2(index)+lambda1(index);
        Fac1(k,index)=fac1(index);
    Fac2(k,index)=fac2(index);
    end
  for index = find( iaold==0),
     dlda(k+1,index)=0;
  end;

  %!!!!!!!!!!!!!!!!!!!!!!!!Set op,dt,dtt!!!!!!!!!!!!!!!!!!!!!!!!!!!!!!!!
  dttemp = [dt ];
  for index = 1:4
     if (thoff1(index) - thon1(index))<0
```

```
    if thnew >= thoff1(index)
        if thnew < thon1(index)
            op(index) = 0;
            if thold<thoff1(index)
                dttemp =  [dttemp (thoff1(index)-thold)/w];
            end
        else
            op(index) = 1;
            if thold < thon1(index)
                dttemp =  [dttemp (thon1(index)-thold)/w];
            end
        end
    else
        op(index) = 1;
    end
else
    if thnew < thoff1(index)
        if thnew >= thon1(index);
            op(index) = 1;
            if thold < thon1(index)
                dttemp =  [dttemp (thon1(index) - thold)/w];
            end
        else
            op(index) = 0;
            if thold>thon1(index)
                dttemp = [dttemp (pi/3-thold)/w];
            end
        end
    else
        op(index) = 0;
```

```
            if thold < thoff1(index)
               dttemp =  [dttemp (thoff1(index)-thold)/w];
            end
         end
      end
   end
   dt =  min(dttemp);
      if k~=nsteps
         dtt = (period - t(k) - dt)/(nsteps-k);
      else
         dtt = (period - t(k) - dt);
      end


% !!!!!!!!!!!!!!!!!!!!!!!!!!!! End Set op,dt,dtt!!!!!!!!!!!!!!!!!!!!!!!!!!!!

   for index=1:4
      if iaold(index)>=ihi,
         va(index)=-vdc;
      end;
      if iaold(index)<=ilo,
         va(index)=vdc;
      end;
      if iaold(index)<ihi,
         if iaold(index)>ilo,
            if diaold(index)>0,
               va(index)=vdc;
            else,
               va(index)=-vdc;
            end;
```

```
            end;
        end;
    end;
    for index=find(op==0)
        if iaold(index)>0,
            va(index)=-vdc;
        end;
        if iaold(index)<=0,
            va(index)=0;
            iaold(index)=0;
        end;
    end;
   dianew=(va-iaold*r-dlda(k+1,:)*w)./dldc(k+1,:);
    Dianew=[Dianew dianew];
    ianew=iaold+dianew*dt;
    for index=find( ianew<0),
       if iaold(index)>0,
          dt =  iaold(index)*dt./(iaold(index)-ianew(index));
          ianew=iaold+dianew*dt;
           if k~=nsteps
              dtt = (period - t(k) - dt)/(nsteps-k);
           else
              dtt = (period - t(k) - dt);
           end
       end;
       ianew(index)=0;op(index)=0;
end;
    dttemp = [dt];

    for index=find(ianew>ihi)
```

```
            if iaold(index)<ihi,
            dt =  (ihi-iaold(index))*dt/(ianew(index)-iaold(index));
            ianew(index)=ihi;
            ianew=iaold+dianew*dt;
            if k~=nsteps
               dtt = (period - t(k) - dt)/(nsteps-k);
            else
               dtt = (period - t(k) - dt);
            end
            va(index)=-vdc;
            %swfac(index)=-1;
         end;

end

for index=find(op)
   if ianew(index)<ilo,
      if iaold(index)>ilo,
         dt=(ilo-iaold(index))*dt/(ianew(index)-iaold(index));
         ianew(index)=ilo;
         ianew=iaold+dianew*dt;
         if k~=nsteps
            dtt = (period - t(k) - dt)/(nsteps-k);
         else
            dtt = (period - t(k) - dt);
         end
         va(index)=vdc;
         %swfac(index)=-1;
      end;
   end;
```

```
 end;
 %dt =  min(dttemp);
 %    if k~=nsteps
 %        dtt = (period - t(k) - dt)/(nsteps-k);
 %    else
 %        dtt = (period - t(k) - dt);
 %    end
%ianew=iaold+dianew*dt;

 t(k+1)=t(k)+dt;
 for index=find(op)
     if ianew(index)>0,
         tcon=tcon+dt;
         tconb=tcon/period;
     end;
 end;

 Swfac=[Swfac swfac'];
 accdcv=swfac.*va.*(iaold+ianew)*dt/2+accdcv;
 pavgdc(k+1,1:4)=accdcv/t(k+1);
for index=1:4
    lambtest=va(index)+ianew(index)+iaold(index);
    if lambtest==0
        lamb(k,1,index)=0;
    else
        if 0<threl(index)
            if threl(index)<=45*pi/180
                lamb(k+1,1,index)=(swfac(index)*va(index)-
(ianew(index)+iaold(index))*r/2)*dt+lamb(k,1,index);%ianew(index)
            else
```

```
                lamb(k+1,1,index)=1.8;%lmin*i(k+1,index);
            end
        end
    end
    poutinst(k+1,index)=ianew(index)*(lamb(k+1,1,index)-lamb(k,1,index))/dt;

avgpout(index)=avgpout(index)+(ianew(index)+iaold(index))*(lamb(k+1,1,index)-
lamb(k,1,index))/2;
    pout(k+1,index)=avgpout(index)/t(k+1);
avgpout2(index)=avgpout2(index)+(ianew(index)+iaold(index))*(lamb(k+1,3,index
)-lamb(k,3,index))/2;
    pout2(k+1,index)=avgpout2(index)/t(k+1);
 end
  i(k+1,:)=ianew;
  e(k+1,:)=dlda(k+1,:)*w;
  pwr(k+1,:)=0.5*e(k+1,:).*ianew;
  v(k+1,:)=swfac.*va;
  iaold=ianew;
  diaold=dianew;
  rms=ianew.*ianew*dt+rms;
  avg=pwr(k+1,:)*dt+avg;
  irms(k+1,:)=sqrt(rms/t(k+1));
  pavg(k+1,:)=avg/t(k+1);
  ps(k+1,:)=va.*ianew;
  idc(k+1,:)=(swfac.*va.*ianew)/vdc;
  accidc=accidc+(idc(k,:)+idc(k+1,:))*dt/2;
  avgidc=accidc/t(k+1);
  thold=th;
  th=th+w*dt;
  threl=[threl(1)+w*dt threl(2)+w*dt threl(3)+w*dt threl(4)+w*dt];
```

```
  if th>pi/3,
     th=th-pi/3;
     kth(2)=1;
     thnext=rpos(kth(2)+1);
  end;
  for index = find(threl>pi/3)
       threl(index)=threl(index)-pi/3;
       kth(index) = 1;
   end
  thnew=th;
  if th>thnext,
     kth=kth+1;
     thnext=rpos(kth(2)+1);
  end;
for index = 1:4
      if iaold(index)<thresh,
         kc(index)=1;
      else,
         kc(index)=fix((iaold(index)-thresh)/deltai)+2;
      end;
      if kc(index)>=ncur-1,
         kc(index)=ncur-1;
      end;
  end
  dldc(1,:)=dldc(2,:);
  swtchfac(k+1,:)=swfac;
  dt=dtt;
  swfac=[1 1 1 1];
  theta(k+1)=th;
  Dt=[Dt dt];
```

```
end;
x0(1:4)=ianew;x0(5:8)=dianew;
lam0=lamb(end,3,:);
avgpout=avgpout*w/nc/2/pi;
pout=[pout,poutinst,pout2];
lamb(1,3,:)=lamb(nsteps+1,3,:);
lamb(1,1,:)=lamb(nsteps+1,1,:);
x0=[iaold'; diaold'];
bifur=[bifur pout2(end,1)]
Irms=[Irms irms(end,1)]
```

VITA

James Thomas Cox III was born in Corbin, KY on June 25, 1952. He attended Corbin Public Schools from the first through the eleventh grade. He graduated from Butler High School in Louisville, KY in 1970. After high school, he attended United Electronics Institute in Louisville, graduating as an electronics technician in 1972. From there, he went to work at Zenith Radio Corporation in Springfield, MO from 1972 to 1975. There, he met and married the former Vicki Ann Daugherty. In 1975, he left Zenith and joined the United States Air Force and served from 1975 to 1978. While stationed at Shepherd Air Force Base in Wichita Falls, TX, his oldest children, Dustin Thomas and Shannon Christine were born. While in Texas, he attended and graduated from Wayland Baptist University with a Bachelor of Science in Occupational Education. After being honorably discharged in 1978, he began a career at Y12 National Security Complex, the Department of Energy plant in Oak Ridge, TN. In 1982, the youngest of his three children, Erin Suzanne was born in Oak Ridge. Since 1978, he has been employed at Y12 as an electronic technician, a health and safety instructor, and an engineer. He received a Bachelor of Science in Electrical Engineering in December of 1997 and a Master of Science in Electrical Engineering in May of 2002 from the University of Tennessee.

James currently lives in Clinton, TN with his wife Vicki and their daughter Erin. He is still employed at the Y12 National Security Complex in the Facility Design Engineering Department of the Engineering and Technology Division as an Instrumentation Engineer.